J. Fluid Mech. (1976), *vol.* 75, *part* 3, *pp.* 553–576
Printed in Great Britain

The generation of sound by two-phase nozzle flows and its relevance to excess noise of jet engines

By O. J. WHITFIELD† AND M. S. HOWE
Engineering Department, University of Cambridge

(Received 1 December 1975)

This paper describes a prototype model experiment designed to test the principle that the 'excess' noise of a jet issuing from a conical nozzle can be significantly diminished by reducing the maximum pressure gradient in the flow. The experiment uses a water jet containing flow inhomogeneities in the form of air or helium bubbles exhausting through a conventional conical nozzle or a specially contoured 'bellmouth' nozzle. It is argued that the level of the internally generated noise is controlled by the mean-flow pressure gradient, and substantial reductions in the sound level are recorded with the bellmouth nozzle. Certain features of the acoustic pressure signatures of the two-phase flow are examined in detail, in particular a rather surprising absolute difference in the sound pressure levels produced when helium rather than air bubbles are used under otherwise identical mean-flow conditions. Theoretical arguments are advanced which appear to explain the principal features of the observations.

1. Introduction

The 'excess' noise generated by sources located within a gas turbine engine is thought to constitute a significant portion of the total sound output at low jet Mach numbers. It appears to be intimately related to the combustion processes, the expansion of gases during exothermic reaction in the combustion chamber together with any unsteady fuel addition resulting in pressure fluctuations that eventually propagate from the jet nozzle as sound. Also, since the reaction depends on the turbulent mixing of fuel and air, pressure fluctuations can arise in the downstream flow because of the unsteady convection of inhomogeneities in entropy and vorticity.

The importance of combustion-associated noise sources is supported by the recent work reported by Hoch & Hawkins (1973) and Whitfield (1975) on the Rolls Royce Olympus engine. Candel (1972), Cumpsty & Marble (1974) and Pickett (1974) have examined analytically the particular case of the noise generated when inhomogeneities, modelled by a train of harmonic entropy and vorticity waves, convect through regions of rapidly varying mean flow such as

† Present address: Mechanical Engineering Laboratory, G.E.C. Power Engineering, Cambridge Road, Whetstone, Leicestershire.

a turbine row. There appears to be no experimental evidence which indicates the importance of this noise generation mechanism compared with that associated with the combustion process *per se*. However, numerical computations undertaken by Cumpsty (1974) suggest that observed temperature fluctuations of about 2 % (Dils 1973) are sufficient to account for the excess noise of several commercial jet engines.

Ffowcs Williams & Howe (1975) extended the analysis to the case of the noise generated by the low Mach number convection of an entropy 'slug' completely filling a compact section of a nozzle. Howe (1975) has also examined the sound generated when entropy 'spots' and compact turbulent eddies are convected past an obstacle in the flow and through a duct contraction. In all cases the possibility of significant acoustic radiation was shown to depend on the presence of a strong mean-flow pressure gradient, a result also obtained by Morfey (1973) in the case of non-uniform free jet flows. This appears to imply that the importance of such noise sources could possibly be significantly diminished by making the maximum pressure gradient of the mean nozzle flow as small as practicable. A conical nozzle has its steepest pressure gradient at the exit. This can be substantially reduced by accelerating the flow uniformly throughout the length of the nozzle by means of an appropriately contoured nozzle wall.

In this paper we describe and attempt to explain a prototype experiment. A low velocity water jet is used, the inhomogeneities being bubbles of gas (air or helium), which generate sound in the pressure gradient of the nozzle flow. Two nozzle configurations are employed. The first is a conical nozzle, in which the pressure gradient has a large maximum at the exit, the second is a specially contoured, or 'bellmouth', nozzle of the same area contraction and length, in which the calculated mean-flow pressure gradient is constant and relatively small.

The results reveal that under nominally identical flow conditions the bellmouth nozzle provides a reduction in the sound pressure level typically of order 10–20 dB. Of course the very large compressibility of the bubbles compared with that of the water flow means that the experiments do not furnish a faithful simulation of an inhomogeneous air jet. Indeed an examination of the acoustic wave profiles suggests that the actual sounding mechanism is associated with the excitation of resonant pulsations of gas bubbles. Although this is different in detail from the dipole type of source mechanism which is thought to be important in inhomogeneous, hot subsonic jets (Morfey 1973), we shall argue below (§ 4) that the intensity of the radiated sound is still determined principally by the magnitude of the pressure gradient.

There are several interesting features of the experimental results which are peculiar to the two-phase nozzle flow. In the case of the conical nozzle the sound pressure level varies approximately as the third power of the mean-flow velocity; for the bellmouth nozzle the exponent was reduced to about 1·5. More surprising, however, was the fact that, although the reduction in sound pressure obtained with the bellmouth nozzle was about the same for both of the gases used, there was a difference of between 5 and 10 dB in the absolute sound pressure levels produced by the two gases under nominally identical flow conditions in the same nozzle.

The magnitude of this difference is too large to be explained by the relatively small difference in the compressibilities of helium and air.

The experimental details and results are described in §§ 2 and 3. In § 4 simple theoretical models are discussed in order to explain the principal features of the observations.

2. Experimental details

A schematic representation of the experimental arrangements is shown in figure 1. Each of the water jets was produced by discharging the domestic water supply from a 13 mm diameter clear plastic pipe through a 4·75 mm diameter nozzle with an area contraction ratio of 7·2. The water flow was throttled and the delivery pressure measured upstream of the point where gas was injected into the flow. Gas was injected at a steady rate over the full range of operating pressures. Downstream the pipe divided into two identical branches supplying the two different nozzles with identical flow mixtures. Details of the nozzles are shown in the inset of figure 1. The first was a straight-walled conical nozzle, while the second, which will be referred to as the 'bellmouth' nozzle, was profiled to produce a uniform flow acceleration. The maximum pressure gradient within the conical nozzle was estimated from the design to exceed that in the bellmouth nozzle by a factor of 6·6 under identical upstream conditions and for an ideal incompressible fluid. Throughout the experiment the volume flow ratio of gas to water at the point of injection was held at a constant value of 0·1.

The jet could be operated satisfactorily over the range of nozzle pressure ratios 1·25–3·0. The corresponding jet velocities were determined in the absence of gas injection from the measured discharge from the nozzle, and were in the range 7–22 m s^{-1}. The jet velocity in the presence of bubbles could not be measured in a straightforward manner, but would generally be expected to exceed that of gas-free flow at the same pressure ratio because of the reduced effective mass density caused by the expansion of the bubbles in the nozzle. An estimate of the velocity can be made if it is assumed that the slip velocity of the bubbles through the water is small. Under these conditions Tangren, Dodge & Seifert (1949) have obtained a modified Bernoulli integral to the one-dimensional equations of two-phase flow, which is discussed in the review article of Wijngaarden (1972, equation (5.4)). This equation has been applied in the present case, and it was found that the difference between the velocity observed in the absence of gas injection and that calculated in this way was less than 8 %, the maximum discrepancy occurring at the lowest pressure ratio.

The experiments were conducted in the open air in order that the jet might be discharged onto a soft surface, so reducing the background noise and the possibility of sound reflexion. The noise was measured by means of a $\frac{1}{2}$ in. Bruel & Kjaer microphone positioned at 90° to the jet axis at a distance of 100 nozzle exit diameters. A typical sample illustrating the form of the measured far-field pressure is shown in figure 2. The noise was dominated by sporodic events in the form of oscillatory pulses, presumably caused by bubbles convecting through the nozzle. These pulses were separated by a random time interval of

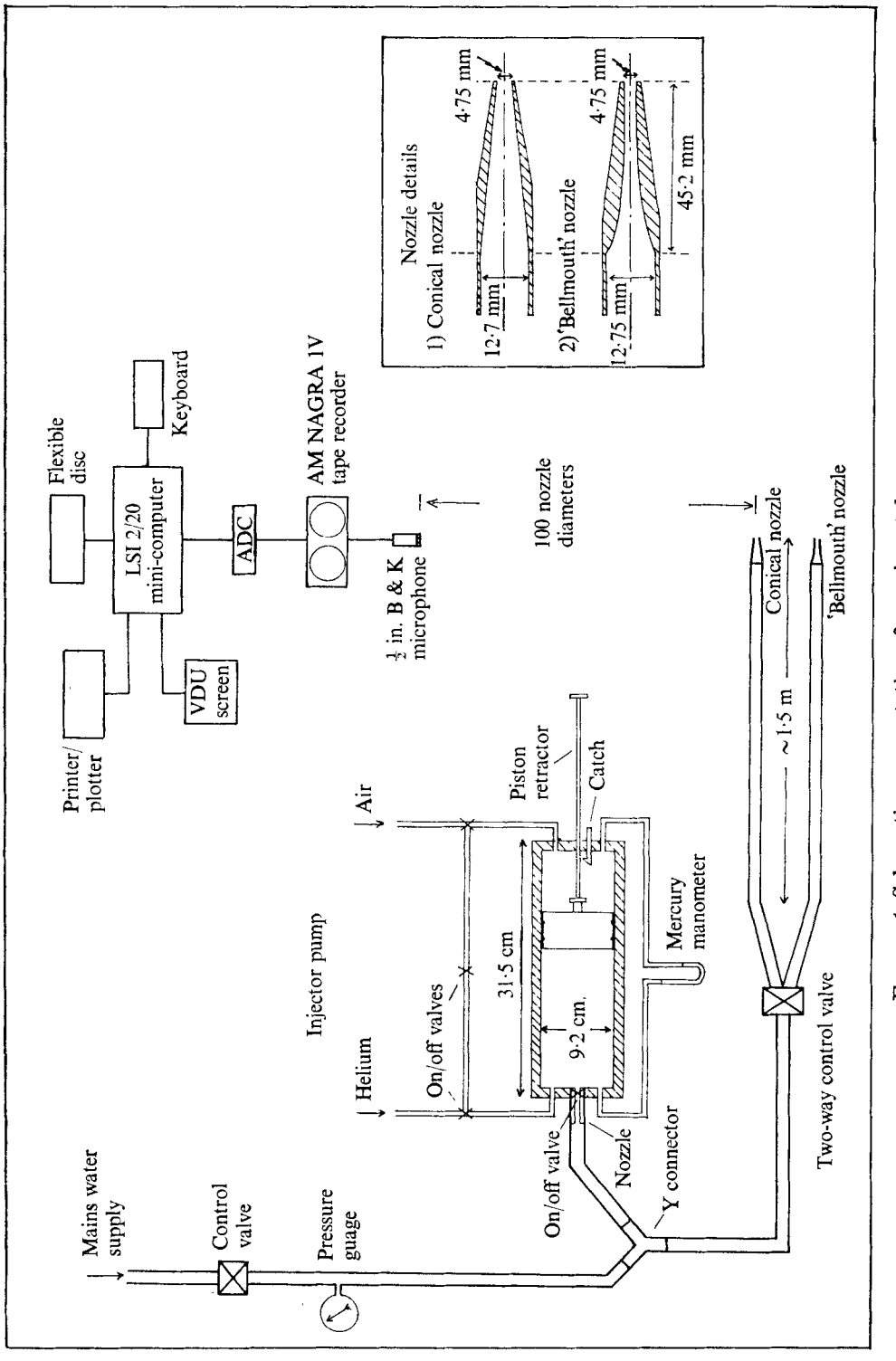

FIGURE 1. Schematic representation of experimental arrangements.

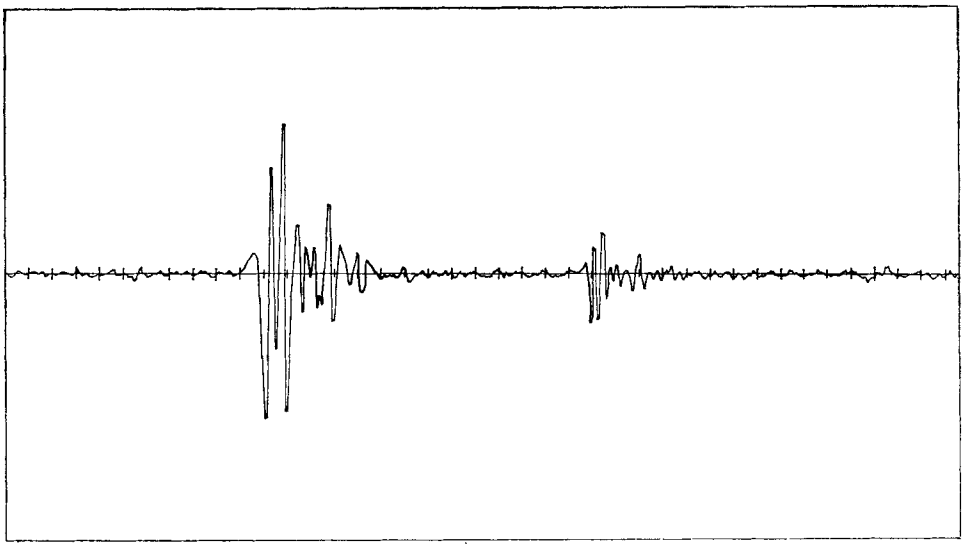

FIGURE 2. Illustrating the sporadic nature of the dominant acoustic events and their magnitude relative to background noise. Each division corresponds to a time interval of 0·1 ms.

2–10 ms, which was generally large compared with the duration of a pulse (0·5–1·0 ms). The intermittent nature of these events indicated that it would be sensible to analyse the data with conditional sampling.

If it is the case that each pressure pulse is associated with the passage of a bubble into the nozzle, the observed oscillatory character suggests that the dominant sound was generated by volume pulsations of the bubbles. Thus it was important to ensure that the decaying oscillatory tail of a recorded pressure signature was indeed a feature of the acoustic signal rather than a reflexion of the response characteristics of the data processing apparatus. The frequencies of the oscillations were in the range 5–10 kHz. No distortion of the signal was expected to be produced by the $\frac{1}{2}$ in. Bruel & Kjaer microphone, which had a response uniform to ± 2 dB over the range 6–20 000 Hz. Experimental measurements reported recently by Ffowcs Williams, Simson & Virchis (1975), however, have emphasized that it is important to ensure that the electronic recording equipment is accurately calibrated when transient events are to be analysed. In the present experiments the pressure fluctuations were recorded on a NAGRA IV J A.M. tape recorder, which is specified by the manufacturers to have a uniform response to within $\pm$ 0·3 dB over the range 2·5 Hz–35 kHz. In order to eliminate entirely the possibility of distortion of the signal arising because of a poor low frequency response (which would manifest itself in the form of an oscillatory response to an ideal step wave input) some of the measurements were repeated using a RACAL Store-4 F.M. tape recorder, which has a flat response from 20 kHz down to d.c. It was not possible to detect any difference in the nature of the pressure signatures obtained in this way, and it was concluded that no significant distortion was introduced by the recording system.

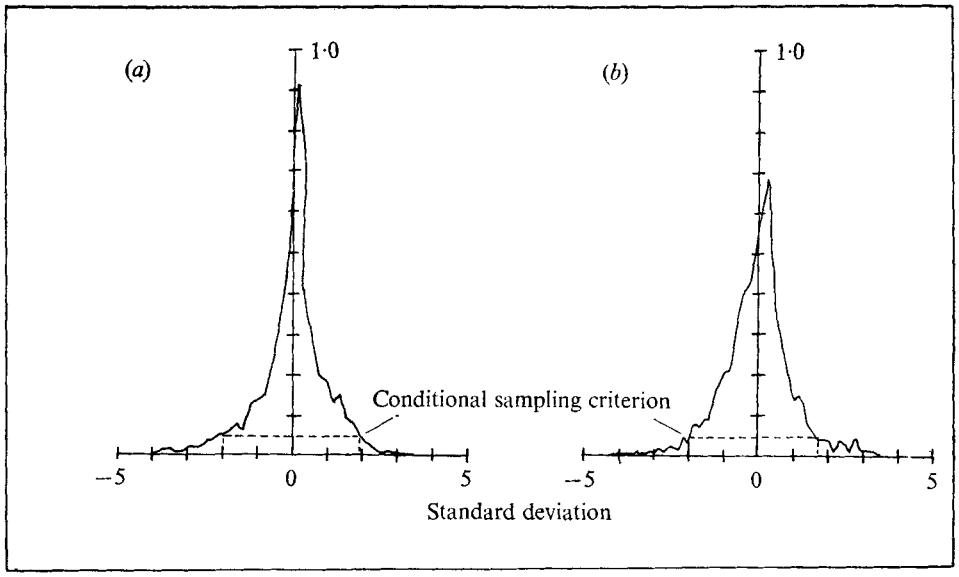

FIGURE 3. Examples of the measured acoustic amplitude probability density functions for a pressure ratio of 3·04 and air injection. The horizontal scale is the amplitude normalized to the standard deviation. (*a*) Conical nozzle. (*b*) Bellmouth nozzle.

3. Experimental results

The sound pressure level of the sporadic events was determined as follows. A pulse was recognized when the unsteady pressure exceeded a certain predetermined level. A suitable sampling time period was chosen to include a portion of the signal both before and after the point of recognition. Any continuing oscillations exceeding a specified amplitude or gradient were also included. A common threshold amplitude was chosen for all experiments. The measured amplitude probability density functions are illustrated for a pressure ratio of 3·04 in figure 3, and were sufficiently similar under all test conditions that the threshold amplitude could be based on a given probability of occurrence; 5 % was the figure chosen. Examples of the conditionally sampled far-field pressure wave forms obtained in this manner are shown in figures 4 and 5. The sound pressure level was deduced from an analysis of a continuous string of these separate events, the data being averaged over more than 20 separate signatures.

The variation of the sound pressure level has been plotted in figure 6 against the pressure drop across the nozzle normalized by the atmospheric pressure, i.e. against (pressure ratio -1), for both nozzles. This mode of presentation of the data, rather than one in which the sound pressure level is plotted against the jet velocity – the usual practice in aerodynamic noise studies – was adopted because of the uncertainty noted in the previous section as to the variation of the two-phase jet velocity with the pressure ratio. In the case of the conical nozzle with helium injection the sound pressure level was proportional to the normalized pressure drop to the power 1·7. The data points for air injection into the conical-

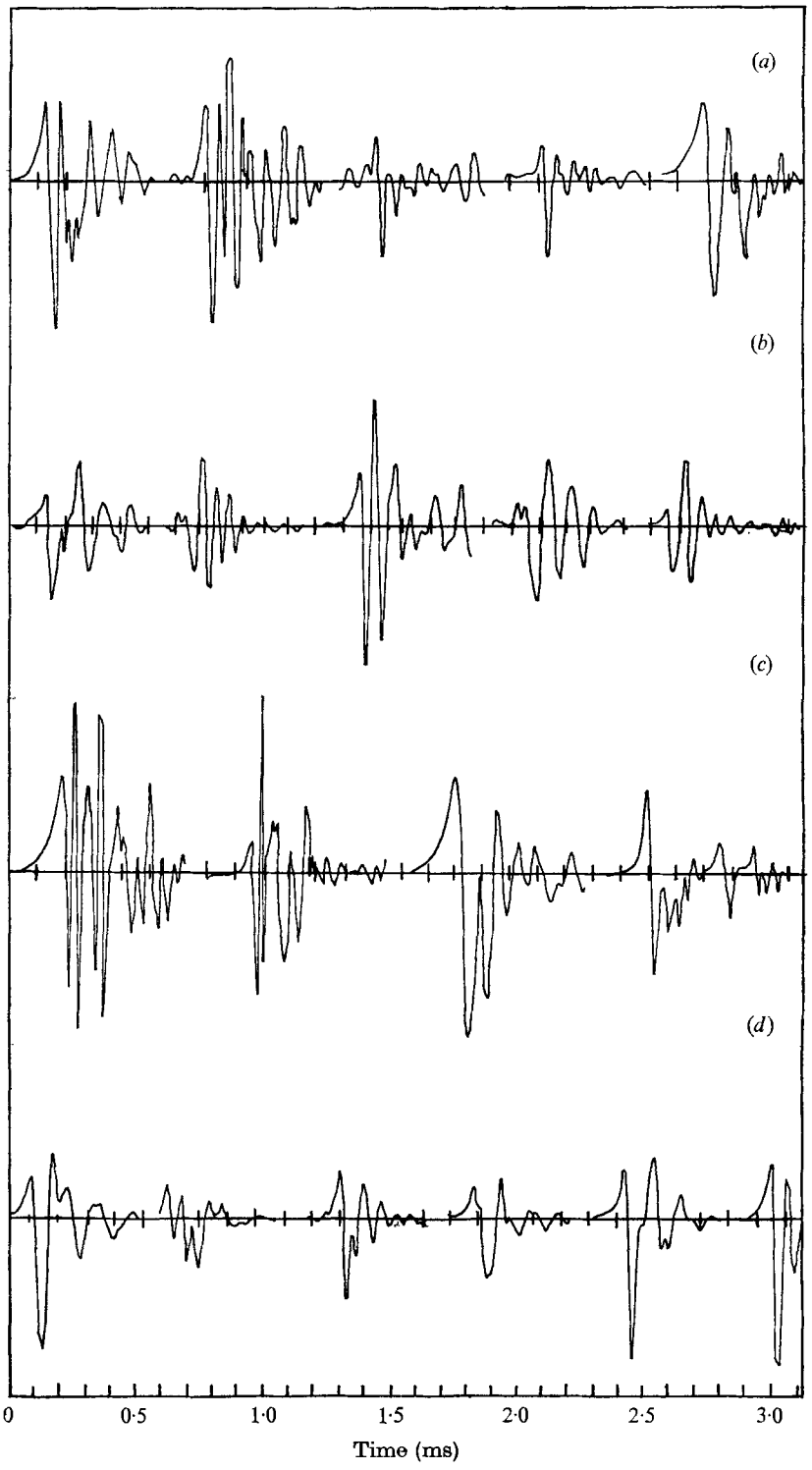

FIGURE 4. Examples of conditionally sampled acoustic wave forms for the conical nozzle. (*a*) Air injection, pressure ratio = 1·68. (*b*) Helium injection, pressure ratio = 1·68. (*c*) Air injection, pressure ratio = 3·04. (*d*) Helium injection, pressure ratio = 3·04.

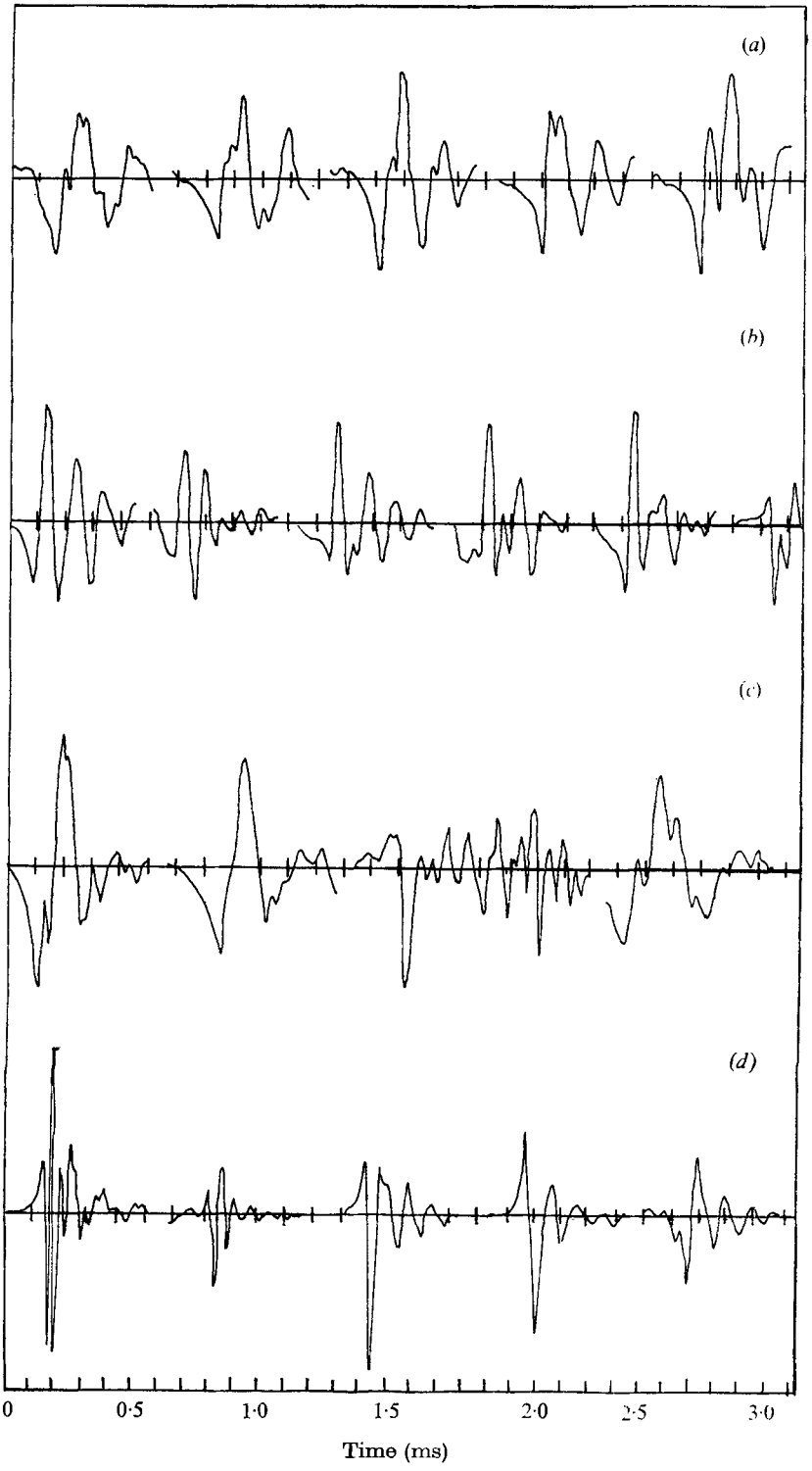

Figure 5. Examples of conditionally sampled acoustic wave forms for the bellmouth nozzle. (*a*)–(*d*) as in figure 4.

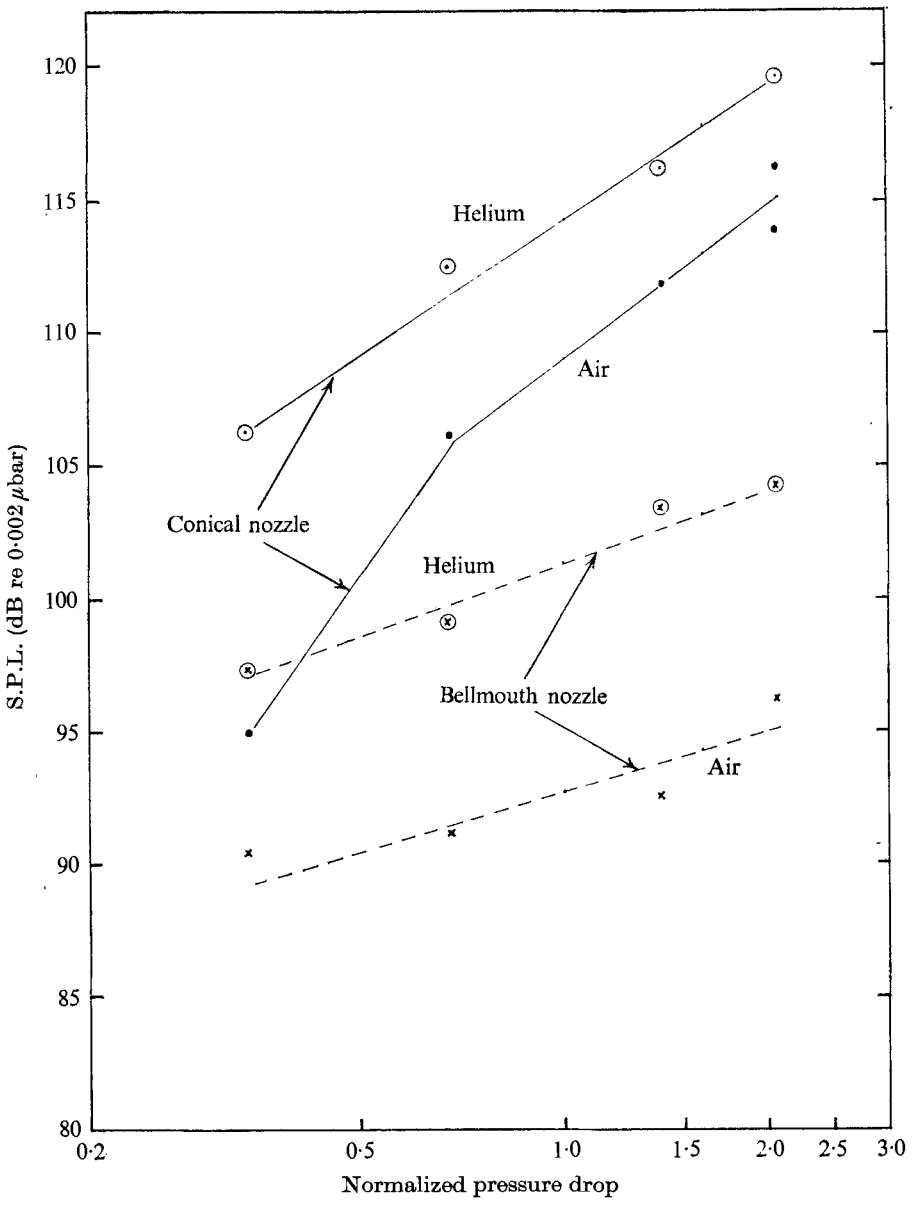

FIGURE 6. The sound pressure level measured at 90° to the jet at a distance of 100 nozzle exit diameters plotted against the pressure drop across the nozzle normalized by the atmospheric pressure.

nozzle flow did not collapse onto a straight line. The experimental point at the lowest pressure ratio in this case was initially thought to be in error, but the measurement was repeated on separate occasions with no detectable difference in the results. The sizes of the bubbles entering the nozzle at the lower pressure ratios were characteristically much larger than those at the higher pressure ratios (cf. the photographs, figures 7 and 8, plates 1 and 2) and this could well imply an

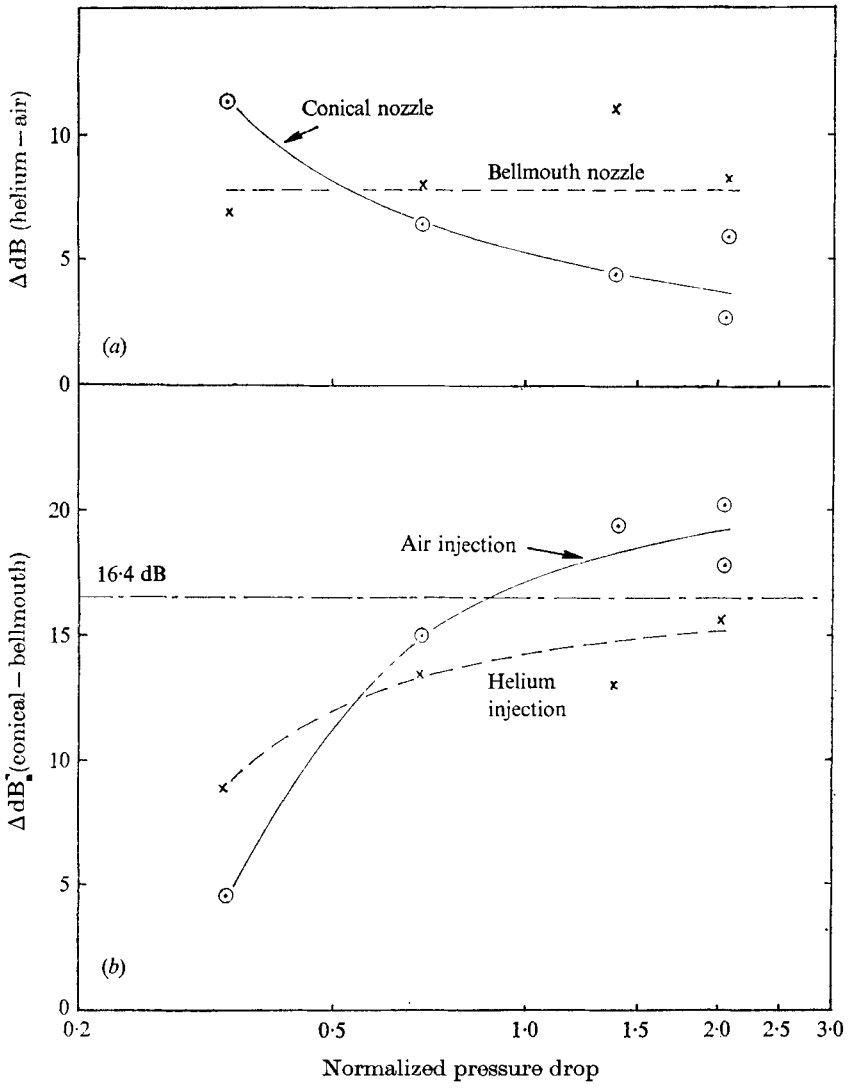

FIGURE 9. (*a*) The difference ΔdB between the sound pressure levels due to helium and air injection. (*b*) Attenuation ΔdB produced by the bellmouth nozzle. The 16·4 dB line is the approximation to the attenuation predicted by means of a comparison of the maximum mean-flow pressure gradients in the absence of gas injection.

essential difference between the mechanics of the nozzle flows at the lower and higher jet velocities.

The results shown in figure 6 for the bellmouth nozzle indicate that for both helium and air injection the sound pressure level was proportional to the normalized pressure drop to a power between 0·7 and 0·9. It is also apparent from the figure that for both nozzles there is a relatively large difference in the sound levels resulting from helium and air injection under otherwise norminally identical flow conditions. The helium bubbles were subjectively much noisier, and the measured

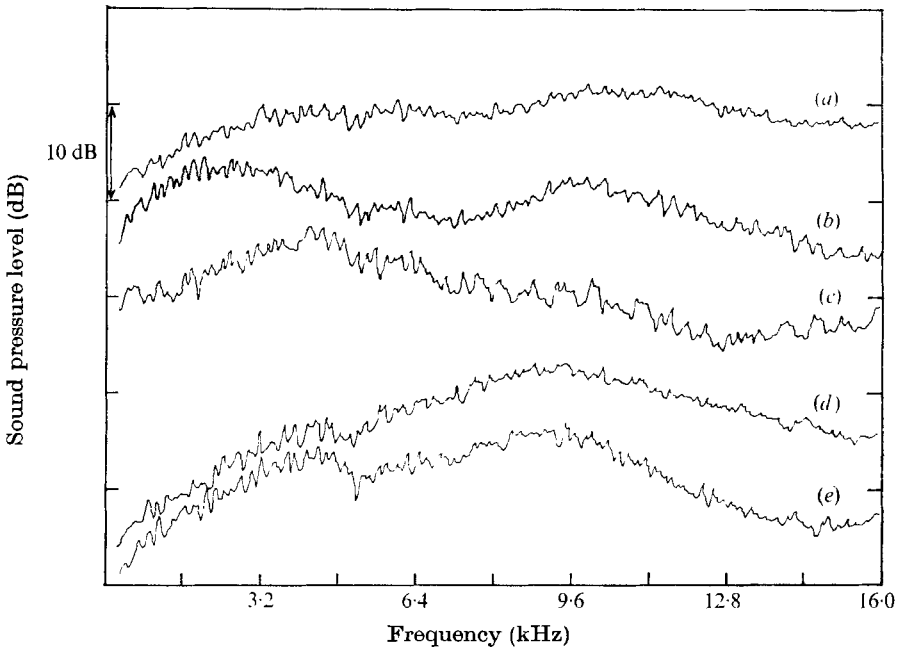

FIGURE 10. Examples of the measured power spectral density of the continuous (i.e. without conditional sampling) acoustic signal. Only the variation of each spectrum is shown; no absolute comparison can be made. (*a*) Conical nozzle, pressure ratio = 3·04, helium. (*b*) Conical nozzle, pressure ratio = 1·68, helium. (*c*) Bellmouth nozzle, pressure ratio = 1·68, helium. (*d*) Conical nozzle, pressure ratio = 3·04, air. (*e*) Bellmouth nozzle, pressure ratio = 3·04, air.

differences for the two nozzles are shown in figure 9 (*a*). Comparison of the sound levels of the two nozzles for the same gas injection shows that the bellmouth nozzle produced a 15–20 dB attenuation for identical upstream flow conditions. The detailed comparison is shown in figure 9 (*b*).

The character of the conditionally sampled wave forms illustrated in figures 4 and 5 is the same for both nozzles, which suggests that the noise generation mechanism is the same in both cases. The pressure first exhibits a transient rise (positive or negative) presumably associated with the passage of a bubble through the increasing pressure gradient of the nozzle. The time scale of this transient was extracted from a detailed examination of a large number of signatures. If it is tentatively assumed that the jet velocity is not significantly different from that measured in the absence of gas injection, and the possible limitations of this assumption have already been mentioned in the previous section, it is found that the time scale is inversely proportional to the jet velocity, the proportionality constant being a length equal to 3–5 % of the nozzle contraction length in all cases.

Following the initial pressure rise there generally occurred a large amplitude decaying oscillation whose duration was typically 0·5 ms, the characteristic period of the oscillation being about 0·1 ms. For pressure ratios greater than 1·7 the frequency of the oscillation appeared to attain an essentially constant value

of about 10 kHz, independent both of the nozzle used and the gas injected. An examination of a large number of the sampled wave profiles also indicated the presence of a smaller characteristic frequency of about 5 kHz when the bellmouth nozzle was operated at the lower pressure ratios (cf. figures 4 and 5). The photographs of the bubble distribution upstream of the nozzle (figure 7) show that at a pressure ratio of 1·68 the two-phase flow consisted of a distribution of large and small bubbles. It is likely that the different observed acoustic frequencies are associated with the range of bubble sizes. The bubbles must disintegrate in the nozzle to form smaller bubbles if the observed frequencies are to correspond to their resonant pulsations (see § 4). At the highest pressure ratio which was examined (3·04), the photographs in figure 8 reveal that the bubbles were smaller, typically 1·5–2 mm in diameter, and the two-phase flow more homogeneous. These views are supported to some extent by a spectral analysis of the *continuous* acoustic signal (figure 10), rather than the conditionally sampled signal. The random occurrence of the oscillatory pulses and the decay of the individual oscillations produced a broad spectrum. However the spectral peak is indicative of the predominant period of oscillation, and occurs at about 9·6 kHz at the higher pressure ratios, a shift to lower frequencies being perceptible for the bellmouth nozzle as the pressure ratio is reduced.

4. Discussion of results

4.1. *Attenuation produced by the bellmouth nozzle*

It was noted in the introduction that model-problem calculations indicate that the amplitude of internally generated sound is linearly proportional to the maximum mean-flow pressure gradient. The design characteristics of the nozzles can therefore be used to obtain a first estimate of the attenuation produced by the bellmouth nozzle. For irrotational incompressible flow the calculated maximum pressure gradient within the conical nozzle exceeded that in the bellmouth nozzle by a factor of 6·6. It follows from this that the attenuation produced by the bellmouth nozzle should be of order $20\log_{10}(6{\cdot}6) \simeq 16{\cdot}4$ dB. Of course the ratio of the mean pressure gradients in the presence of two-phase flows must differ from the above value, but an approximate analysis of the type mentioned in § 2 indicates that the effect is to reduce the above prediction only by about 1 dB and 2·5 dB at respectively the lowest and highest pressure ratios examined.

These estimates of the attenuation are in reasonable order-of-magnitude agreement with the observed levels of figure 9 (*b*) for pressure ratios greater than about 1·7. The characteristic frequency of the sporadic, oscillatory acoustic pulses tended to be much lower for the bellmouth than for the conical nozzle at the lower pressure ratios. This may account for the large discrepancy between figure 9 (*b*) and the predicted attenuation at the lower pressure ratios, since a proper theoretical comparison of the nozzles should also take account of the unknown frequency dependence of the sound levels.

4.2. *Sound generation mechanisms*

In this subsection we shall derive expressions which enable us to estimate that a bubble pulsating resonantly at a frequency of 5–10 kHz must have a radius of about 0·35–0·7 mm. This is rather smaller than the typical size of a bubble shown entering a nozzle in the photographs in figures 7 and 8. These bubbles might well disintegrate as they enter the nozzle flow, a feature made probable by their relatively high Weber number, which is characteristic of a structurally unstable bubble (Wallis 1969, p. 247). Thus we are led to postulate that a resonant bubble pulsation can be induced following: (*a*) the impulsive disintegration of a large bubble; (*b*) the formation of the smaller bubbles which subsequently convect through the relatively large pressure gradient at the nozzle exit.

We shall examine a simplified model of case (*b*) first. Consider a spherical bubble whose radius is much smaller than the length characterizing the variations in the mean flow and which is convected along the axis of the nozzle. The bubble will remain spherical if it is sufficiently small and we shall assume further that the ambient flow in the neighbourhood of the bubble may be assumed to be potential. Thus effects associated with the presence of a turbulent wake are specifically excluded.

Take the x axis along the axis of the nozzle, and let $x_0(t)$ denote the position of the centre of the bubble at time t, and $V = dx_0/dt$ the bubble velocity. In a first approximation the perturbation pressure within the bubble is given by

$$p = p_0(t) - \rho_1 (dV/dt)\, r \cos\theta, \tag{4.1}$$

where ρ_1 is the density of the gas and (r, θ) are spherical polar co-ordinates with origin at the instantaneous location of the centre of the bubble, θ being measured from the direction of motion. The first term on the right of (4.1) accounts for uniform pressure fluctuations arising from changes in the bubble volume; the second term is associated with the small pressure gradient required to produce a uniform acceleration dV/dt of the gas within the bubble.

Let v denote the spherically symmetric pulsation velocity of the bubble surface. This can be related to the component $p_0(t)$ of the pressure by making use of the continuity equation, which we write in the form

$$\frac{1}{\rho_1 c_1^2}\frac{Dp}{Dt} + \operatorname{div}\mathbf{v} = \frac{1}{c_p}\frac{DS}{Dt}. \tag{4.2}$$

Here $\mathbf{v}$ and S denote respectively the gas velocity and specific entropy, and c_1 is the sound speed in the gas and c_p the specific heat at constant pressure. The term on the right of (4.2) is absent when dissipation within the bubble is neglected. However, this term must be retained if it is desired to account quantitatively for the observed decay of the acoustic wave profiles. Devin (1959) and Chapman & Plesset (1970) have examined the relative contributions of viscosity, heat conduction and acoustic radiation to the damping of resonant pulsations of a bubble, and concluded that for the frequencies important in the present context the most important energy loss mechanism is thermal conduction. In the case of a convected bubble there is also likely to be additional dissipation arising from a

fluctuating viscous drag, analogous to that examined by Batchelor (1969). However experiments by Macpherson (1957) and Silberman (1957) on the propagation of sound through a bubbly medium in which the bubble size was controlled with great accuracy indicated that the principal dissipation mechanism was still that of thermal conduction within the bubble.

Integrate (4.2) over the volume of the bubble to obtain

$$\frac{1}{\rho_1 c_1^2}\frac{Dp_0}{Dt}+\frac{3v}{a}=\frac{3}{4\pi a^2}\int\frac{1}{c_p}\frac{DS}{Dt}\,d^3\mathbf{x}. \tag{4.3}$$

In writing down this result we have linearized conditions about a mean bubble size, which is assumed for the purposes of the present calculation to be constant, the mean radius being denoted by a. The integral on the right-hand side may be determined from the linearized energy equation

$$\frac{1}{c_p}\frac{DS}{Dt}=\frac{\chi}{T_0}\nabla^2 T, \tag{4.4}$$

where T_0 and T denote respectively the mean-flow temperature (assumed constant) and the fluctuation temperature of the gas in the bubble; χ denotes the thermometric conductivity of the gas. Integrating (4.4) over the bubble and making use of the divergence theorem then permits one to write (4.3) in the form

$$\frac{1}{\rho_1 c_1^2}\frac{Dp_0}{Dt}+\frac{3v}{a}=\frac{3\chi}{aT_0}\left(\frac{\partial T}{\partial r}\right)_{r=a}, \tag{4.5}$$

where only the spherically symmetric component of the temperature fluctuation contributes to the right-hand side. This contribution may be calculated as follows.

Assuming ideal-gas behaviour and a harmonic time dependence $\exp(-i\omega t)$, the spherically symmetric temperature fluctuation satisfies (4.4) expressed in the form

$$\frac{1}{r}\frac{\partial^2}{\partial r^2}(rT)=-\frac{i\omega}{\chi}\left(T-\frac{p_0}{\rho_1 c_p}\right). \tag{4.6}$$

Note that in (4.6) the variation with r of the spherically symmetric pressure component resulting from the effect of heat conduction has been ignored. A more detailed analysis reveals that such variations are confined to a thin boundary layer of width $\sim(\chi/\omega)^{\frac{1}{2}}$ at the interior surface of the bubble and have a relative magnitude of order $\omega\chi/c^2$, which is very small for the values of the radian frequency ω of interest. Equation (4.6) is easily solved by noting that to a very good approximation the relatively large heat capacity of water implies that the temperature fluctuation at the surface of the bubble is negligibly small. Thus we find that

$$T=\frac{p_0}{\rho_1 c_p}\left\{1-\frac{a\sin(\sigma r)}{r\sin(\sigma a)}\right\}, \tag{4.7}$$

where

$$\sigma^2=i\omega/\chi. \tag{4.8}$$

If Γ is defined by

$$\Gamma=1-\sigma a\cot(\sigma a), \tag{4.9}$$

then the substitution of (4.7) into (4.5) leads to the following relation between harmonic variations of p_0 and the bubble pulsation velocity v:

$$v = \frac{a}{3\rho_1 c_1^2}\left\{i\omega + \frac{3\chi(\gamma-1)\,\Gamma}{a^2}\right\}p_0, \tag{4.10}$$

where γ is the ratio of the specific heats of the gas. This result shows that v has a component dependent on the thermal characteristics of the gas which is in phase with the pressure p_0, indicating that the bubble behaves as a net sink of mechanical energy.

When the bubble convects in the nozzle the mean-flow pressure gradient causes the bubble to accelerate relative to the water and to change in volume. In order to examine these effects we suppose that the ambient flow in the immediate neighbourhood of the bubble may be regarded as incompressible, a condition which requires the wavelength of the radiated sound to be much larger than the bubble radius. In the absence of the bubble the flow is specified by a steady velocity potential $\phi_0(\mathbf{x})$, say. Let $U = (\partial\phi_0/\partial x)_{x_0}$, the mean-flow velocity evaluated at the location of the centre $x_0(t)$ of the bubble, and $U' = (\partial^2\phi_0/\partial x^2)_{x_0}$. Then it is easily verified that close to the bubble the potential may be expanded in the form

$$\phi = \phi_0(\mathbf{x}) - \frac{va^2}{r} + \frac{(U-V)}{2r^2}a^3\cos\theta + \frac{U'a^5}{3r^3}P_2(\cos\theta) + \ldots, \tag{4.11}$$

where the terms omitted are negligible provided that changes in the mean flow are small over a distance of the order of the bubble radius.

Variations in the mean bubble radius produce second-order effects in the perturbation terms of (4.11) and are neglected. Thus in the linear approximation it is readily deduced from Bernoulli's theorem that the variable part of the ambient pressure on the surface of the bubble is given by

$$p = \rho_0\{a\,dv/dt - \tfrac{1}{2}[U^2 + \tfrac{1}{2}(U-V)^2]\} + \{\rho_0\,dV/dt + 3(\partial p/\partial x)_{x_0}\}a\cos\theta + \ldots, \tag{4.12}$$

where $(\partial p/\partial x)_{x_0} \equiv -\rho_0 UU'$ is the mean-flow pressure gradient evaluated at $x_0(t)$, ρ_0 being the density of water, or more generally of an ambient two-phase flow.

For bubble radii greater than about 0·02 mm, surface tension makes an insignificant contribution to the gas pressure and corresponding terms in (4.1) and (4.12) may be equated to give

$$p_0(t) - a\rho_0\,dv/dt = -\tfrac{1}{2}\rho_0\{U^2 + \tfrac{1}{2}(U-V)^2\}, \tag{4.13}$$

$$(2\rho_1 + \rho_0)\,dV/dt = -3(\partial p/\partial x)_{x_0}. \tag{4.14}$$

The second of these equations describes the motion of the bubble along the axis of the nozzle. Since $\rho_1 \ll \rho_0$ (4.14) expresses the well-known result that the acceleration experienced by the bubble is three times that of the ambient fluid it displaces (Batchelor 1967, p. 455).

Since the pulsation velocity v is related to p_0 by (4.10) for harmonic variations, it follows that (4.13) determines the dependence of the mean bubble pressure p_0 on the variations in the ambient dynamic pressure $-\frac{1}{2}\rho_0[U^2 + \frac{1}{2}(U-V)^2]$. This

pressure is a function of the position of the bubble, i.e. of time, so that it may be regarded as a Fourier composition of harmonic components $\mathscr{P}e^{-i\omega t}$, say. For each such component (4.13) and (4.10) can be combined to yield a single equation for p_0:

$$\left\{\omega^2 - \frac{3i\chi(\gamma-1)\,\Gamma\omega}{a^2} - \omega_0^2\right\} p_0 = -\omega_0^2 \mathscr{P}, \tag{4.15}$$

where ω_0 is the *adiabatic* resonance frequency of the bubble, defined by

$$\omega_0^2 = 3\rho_1 c_1^2/\rho_0 a^2. \tag{4.16}$$

The zero of the term in curly brackets on the left of (4.15), regarded as a function of ω, defines the actual resonance frequency of the bubble pulsations. When heat conduction is ignored, so that the bubble behaves adiabatically, $\omega = \omega_0$, a result first obtained by Minnaert (1933). The importance of heat conduction is determined by the dimensionless parameter

$$\sigma a \equiv a(i\omega/\chi)^{\frac{1}{2}}, \tag{4.17}$$

which is the ratio of the mean bubble radius to the thermal length scale $(\chi/\omega)^{\frac{1}{2}}$.

The observed values of the characteristic frequencies (5–10 kHz) and the above results may be used to confirm that in the present case σa is expected to be large, and that the radian frequency at resonance of the bubble pulsation is given approximately by

$$\omega = \omega_0(1 - i\delta), \tag{4.18}$$

where

$$\delta = \frac{3(\gamma-1)}{2a}\left(\frac{\chi}{2\omega_0}\right)^{\frac{1}{2}}. \tag{4.19}$$

The coefficient δ determines the decay of the oscillation, and is such that the wave amplitude is diminished by a factor of $1/e$ over a period of time equivalent to $1/(2\pi\delta)$ oscillations. Note that (4.18) and (4.19) include no effect of the nozzle walls nor of the free jet surface. This is consistent with the assumption that the bubble radius is small compared with the nozzle length scale, but it may also be noted that Strasberg (1953) has shown that surface effects modify the above conclusion by more than about 10 % only when the bubble is located closer than a bubble diameter to the surface.

Since dissipation is important only near to resonance we may now approximate the second term in the curly brackets of (4.15) by evaluating Γ at $\omega = \omega_0$. It then follows that the real-time equation governing the variations in the mean bubble pressure p_0 is approximately

$$\frac{D^2 p_0}{Dt^2} + 2\omega_0\delta\frac{Dp_0}{Dt} + \omega_0^2 p_0 = -\tfrac{1}{2}\omega_0^2\rho_0[U^2 + \tfrac{1}{2}(U-V)^2]. \tag{4.20}$$

This result shows that resonant pulsations can be excited in the bubble provided that the variations in the dynamic pressure on the right of (4.20) have a significant spectral component in the neighbourhood of ω_0. Strasberg (1956) and Hall (1969) have considered analogous models of bubble excitation in a non-uniform mean flow, but took no account of dissipation, nor of the dynamic

pressure variations arising from the slip velocity $V-U$ of the bubble. Actually a resonant response is most likely to be initiated as the bubble leaves the nozzle, where the pressure gradient of the mean flow is greatest. In this case simple order-of-magnitude estimates using (4.14) indicate that a corresponding impulsive variation in the slip velocity results in an impulsive change in the dynamic pressure experienced by the bubble which is always less than about 25 % of that arising from the variation in the mean-flow conditions. It follows, from expressions to be obtained below, that the additional contribution to the acoustic field from the slip-velocity term in (4.20) amounts to about 2 dB.

The formula (4.19) for the decay coefficient may be applied to the experimental pressure profiles. At a temperature of 300 °K the thermometric conductivities of air and helium are respectively 0·22 and 1·77 $\mathrm{cm^2\ s^{-1}}$ at a pressure of one atmosphere. Thus at a frequency of 10 kHz, which is characteristic of the acoustic profiles illustrated in figure 4 for the conical nozzle, it follows from (4.16) and (4.19) that the corresponding bubble radius is about 0·3 mm and that the wave amplitude diminishes by a factor of $1/e$ after about six or seven oscillations in the case of an air bubble and after about $1\frac{1}{2}$–2 oscillations for a helium bubble. These predictions are consistent with many of the observed profiles. The decay of the helium oscillations at this frequency is certainly much more rapid than that of an air bubble. The agreement is particularly good for the air-bubble profiles shown in figure 4. This may therefore be regarded as lending support to our approximation, in which only the effects of heat conduction contribute significantly to the dissipation.

Return now to the question of the excitation of the bubble resonances. In the model problem leading to (4.20) it is clear that a resonance will be excited at a frequency of 5–10 kHz only if the dynamic pressure varies rapidly along the trajectory of the bubble. This occurs where the pressure gradient is large, i.e. at the nozzle exit. Before we examine the consequences of this we shall consider briefly the possibility (*a*) above, of the excitation of a resonance by bubble disintegration.

The tendency of a bubble to break up is governed by the magnitude of the Weber number

$$We = \frac{\rho_0 (U-V)^2}{\Sigma/2a} \tag{4.21}$$

(see, for example, Wallis 1969, p. 247), where Σ is the surface tension. Little authoritative work seems to have been done in this field, but it appears that a bubble is likely to remain intact for We of the order of 10 or less (Hinze 1955). The Weber numbers of the bubbles shown in the photographs (figures 7 and 8) are typically very much greater than this, for example $We \sim 15$–110 for a bubble of radius 1 mm and a slip velocity equal to 10 % of the jet velocity.

The excitation of resonances by the disintegration of a bubble was first examined by Strasberg (1956). Strasberg pointed out that when a bubble splits into two smaller bubbles at constant pressure there is a difference between the equilibrium pressures of the larger and the smaller bubbles which arises because of the increased surface-tension pressure on the smaller bubbles. This is equi-

valent to the application of an impulsive pressure, which appears as a forcing term on the right-hand side of the response equation (4.20), the magnitude of the pressure being of order $2\Sigma/a$. When a bubble breaks up in a nozzle flow, in the presence of a relatively large pressure gradient, resonant pulsations are excited by a second mechanism, which has not apparently been considered hitherto. In this case the parent bubble is stretched in the direction of the ambient pressure gradient. The actual pressure within the bubble is effectively uniform, so that if, for example, the bubble necks and snaps into two near its centre of elongation, resonant pulsations can be induced in the two smaller bubbles by an effective surface pressure analogous to Strasberg's surface-tension pressure and of magnitude $\sim a(\partial p/\partial x)_0$, where a is the bubble radius and $(\partial p/\partial x)_0$ the mean-flow pressure gradient. In order to compare the relative efficiencies of these two mechanisms, consider a bubble of radius $a \simeq 0{\cdot}3$ mm and approximate the value of the largest pressure gradient by a pressure drop of one atmosphere over a distance estimated in § 3 to be of the order of 5 % of the nozzle contraction length shown in figure 1, i.e. of 4·52 cm. The corresponding resonant acoustic response of a bubble is proportional to the impulsive pressure [cf. (4.22) below], and it follows that the ratio of the sound intensity produced by the impulsive pressure-gradient force to that arising from surface-tension effects is of order 25 dB.

4.3. *The intensity of the radiated sound*

The sound generated by a pulsating bubble is ideally represented by a monopole acoustic source. However, when the changes in the volume of the bubble are produced by the mean flow, it is necessary to recall that even in the absence of pulsational oscillation of the bubble there is a change in the mean density of the two-phase flow resulting from the variation in the mean pressure as the fluid flows down the pressure gradient of the nozzle. Thus the strength of the monopole source must involve a factor dependent on the difference between the compressibility $1/\rho_1 c_1^2$ of the gas in the bubble and that of the ambient two-phase flow. Let c_0 denote the sound speed in the bubbly medium. Ffowcs Williams & Howe (1975) have shown that, when the effect of convection on the radiated sound is ignored, the acoustic pressure fluctuations within the flow at a distance R from the bubble are given by

$$p \simeq \frac{\Delta\rho_0}{4\pi R}\left(\frac{1}{\rho_0 c_0^2}-\frac{1}{\rho_1 c_1^2}\right)\left[\frac{D^2 p_0}{Dt^2}\right], \tag{4.22}$$

where $\Delta = \frac{4}{3}\pi a^3$ is the volume of the bubble and the term in square brackets is evaluated at the retarded time $t - R/c_0$. Results analogous to (4.22) have been obtained in a similar context by Strasberg (1956) and Crighton & Ffowcs Williams (1969), although no account was taken of the relative compressibilities of the bubble and the mean flow, the first term in the curly brackets being neglected. That term is not always small, however, since the speed of sound c_0 can attain values considerably smaller than c_1 or the sound speed in pure water for quite moderate bubble concentrations (Wijngaarden 1972).

Two further remarks are necessary to justify the use of (4.22) in the present case. First, the experimental observations were made at an angle of 90° to the jet

axis, so that modifications to the solution due to effects of Doppler amplification (Lighthill 1952) are not present. It is possible, however, that a large slip velocity $V-U$ of the bubble could destroy the simple monopole picture of the source in the manner described very recently by Dowling (1976), but for the small bubbles which are likely to be the important sound sources $V-U$ is probably quite small, and in any case the additional contribution from this term apparently has the undesirable effect of raising the exponent of the parametric dependence of the sound on the normalized pressure drop across the nozzle. Second (4.22) represents the field of a spherical wave radiating into the two-phase flow, no account having been taken of the boundaries of the jet flow nor of the nozzle geometry. This is expected to be an adequate approximation, since the very small sound speed (~ 35 m s^{-1}, according to formulae given by Wijngaarden 1972) within the jet indicates that the relevant acoustic wavelengths are rather small. Further, since acoustic waves decay rapidly in a bubbly medium (Wijngaarden 1972) multiple reflexions are likely to be unimportant, and the formula for the free-space radiation is obtained by multiplying the result (4.22) by an appropriate transmission coefficient, viz.

$$2\rho_s c_s/(\rho_s c_s+\rho_0 c_0) \simeq 2(\rho_s c_s/\rho_0 c_0),$$

where ρ_s and c_s are respectively the free-space density and sound speed.

Thus at a distance R from the nozzle and at 90° to the jet axis the free-space acoustic radiation resulting from bubble pulsations at the resonant frequency ω_0 of (4.16) is given by

$$\frac{p}{p_s} \simeq 2\left(\frac{a}{R}\right)\left\{1-\frac{\rho_1 c_1^2}{\rho_0 c_0^2}\right\}\frac{\gamma_s}{\rho_0 c_0 c_s}[p_0], \tag{4.23}$$

where p_s is the atmospheric pressure and γ_s the ratio of the specific heats of air. It is clear that, since $\rho_1 c_1^2$ is practically the same whether the bubbles are of helium or air, (4.23) contains no terms which can account for the observed 5–10 dB difference between the sound pressure levels of helium and air bubbles shown in figure 9(*a*). This question is examined further below.

The retarded value of the pulsational pressure p_0 appearing on the right of (4.23) may be determined from (4.20). The effect of the dynamic pressure on the right of (4.20) is obtained by assuming that it changes very rapidly at the nozzle exit. The precise rate of change (i.e. the pressure gradient) depends on the nozzle geometry, but in a first approximation it may be supposed to change discontinuously by an amount dependent on the pressure ratio of the jet. If p_J denotes the pressure upstream of the nozzle, it follows from (4.20) that the fluctuating component of p_0 is given by

$$p_0(t) = (p_J-p_s)\exp(-\omega_0\delta t)\cos\omega_0 t \tag{4.24}$$

for $t > 0$, where it is also assumed that the bubble convects through the nozzle exit at time $t = 0$. Thus the sound pressure level varies as the square of the normalized pressure drop, which is somewhat larger than the observed dependence (figure 6) for the conical nozzle, and much larger than that observed for the bellmouth nozzle.

Using these results we can obtain a quantitative estimate of the sound pressure level produced at a distance of 100 nozzle diameters by a single bubble resonating at a frequency of 10 kHz. At a pressure ratio of 1·68 (4.23) and (4.24) predict an acoustic intensity of about 94 dB, this figure rising to 104 dB at the highest pressure ratio 3·04. These are in order-of-magnitude agreement with the results of figure 6.

When a bubble resonance is initiated by the breakup of a larger bubble in the manner already described, a similar analysis shows that the sound pressure level is again proportional to the square of the normalized pressure drop.

One possibility not yet examined is that the two-phase flow in the neighbourhood of the nozzle exit may well lead to a local overexpansion of the mixture (cf. Wijngaarden 1972), so that a bubble finds itself momentarily in a region of reduced pressure. If τ denotes the duration of this overexpansion for a particular bubble, then $\tau \simeq L/U$, where L is a length dependent on the nozzle geometry. If this length characterizes the initial rise of the observed pressure profiles then, with the reservations already discussed in § 3, it is of the order of about 3–5 % of the nozzle length. Let $P \sim \rho_0 U^2$ denote the magnitude of the pressure fluctuation accompanying the overexpansion. The corresponding resonant response of the bubble may be estimated by inserting a forcing term of the form $\omega_0^2 \tau P \delta(t)$ into the right of (4.20), and this leads to a free-space acoustic pressure p given by

$$\frac{p}{p_s} \simeq 2\left(\frac{a}{R}\right)\left\{1-\frac{\rho_1 c_1^2}{\rho_0 c_0^2}\right\}\frac{\gamma_s \omega_0 \tau P}{\rho_0 c_0 c_s}[\exp(-\delta\omega_0 t)\sin\omega_0 t], \tag{4.25}$$

the terms in the square brackets being evaluated at the retarded time $t - R/c_s$.

It has already been noted in § 3 that the resonance frequency ω_0 apparently changed very little for pressure ratios greater than about 1·7. If this is indeed the case it follows from (4.25) that, since $\tau \sim L/U$, the sound pressure level is directly proportional to the normalized pressure drop (i.e. to $\rho_0 U^2$) at the larger pressure ratios. It is difficult to give a reliable quantitative estimate of the sound pressure level because of the uncertainty in the values of the quantities involved, however if P is about 10 % of the atmospheric pressure p_s and $U \sim 15$ m s^{-1}, the level predicted by (4.25) at 100 nozzle diameters is about 97 dB, for a bubble resonating at a frequency of 10 kHz. Again this result is in reasonable agreement with the observations, and the predicted dependence on the pressure drop across the nozzle indicates that this mechanism may well be important in the bellmouth nozzle.

4.4. *Difference between the radiation from helium and air bubbles*

None of the mechanisms examined above is capable of explaining the 5–10 dB difference in the sound pressure levels observed (figure 9*a*) for helium and air bubbles under nominally identical flow conditions. We shall now propose an explanation which depends on the anomalous absorption of sound which can occur in a bubbly medium. To do this we shall assume that the disintegration of a large bubble in the pressure gradient of the nozzle produces a fairly homogeneous bubbly medium in which the characteristic bubble size is compatible with the observed oscillatory frequencies of the acoustic pulses. Thus a resonating

bubble actually radiates into a medium consisting essentially of an assembly of harmonic oscillators. When the acoustic frequency is close to one of the characteristic frequencies of these oscillators the wave is rapidly absorbed.

The question of sound propagation in a bubbly two-phase flow has been extensively studied (e.g. Carstensen & Foldy 1947; Meyer & Skudrzyk 1953; Wijngaarden 1972; Batchelor 1969), although it appears that the only loss mechanism explicitly included in these earlier investigations was that associated with viscous stresses. Actually all theories describe only the propagation of the coherent component of the acoustic field, where the relevant perturbation pressure $\overline{p}$ and velocity $\overline{\mathbf{v}}$ are defined by an average over a region of space small compared with the wavelength yet containing many bubbles. Provided the wavelength is sufficiently large the effect of incoherent scattering is expected to be small compared with that resulting from the averaged dynamic response of the bubbles.

If α denotes the proportion by volume of bubbles present, then in a frame moving with the mean jet velocity the averaged momentum equation is

$$\frac{\partial \overline{\mathbf{v}}}{\partial t} = \frac{-1}{(1-\alpha)\rho}\frac{\partial \overline{p}}{\partial \mathbf{x}}, \tag{4.26}$$

where ρ is the density of water, so that $\rho_0 = (1-\alpha)\rho$. In writing down the averaged equation of continuity account must be taken of a random distribution of sources and sinks formed by the bubbles. If v_n denotes the radial velocity at the surface of a bubble of mean radius a_n, the appropriate continuity equation is

$$\frac{(1-\alpha)}{\rho c^2}\frac{\partial \overline{p}}{\partial t} + \operatorname{div}\overline{\mathbf{v}} = \sum_n \frac{3\alpha_n \overline{v}_n}{a_n}, \tag{4.27}$$

where c is the sound speed in water and α_n is the volume density of bubbles of radius a_n.

The locally averaged perturbation pressure $\overline{p}_n$ within a bubble of radius a_n is related to $\overline{v}_n$ and $\overline{p}$ by

$$\overline{p}_n = \rho a_n \partial \overline{v}_n/\partial t + \overline{p} \tag{4.28}$$

if the effects of surface tension are negligible. For harmonic time dependence $\exp(-i\omega t)$, $\overline{p}_n$ and $\overline{v}_n$ are also related by an equation analogous to (4.10), and when this is used in conjunction with (4.26)–(4.28), it may be shown that $\overline{p}$ satisfies a wave equation of the form

$$\nabla^2 \overline{p} + k^2 \overline{p} = 0, \tag{4.29}$$

where the complex wavenumber k is defined by

$$k^2 = \frac{\omega^2}{c^2}(1-\alpha)^2 + \sum_n \frac{3\alpha_n(1-\alpha)\,\omega^2\{1 - 3i\chi(\gamma-1)\,\Gamma_n/\omega a_n^2\}}{a_n^2\{\omega_n^2 - \omega^2 + 3i\omega\chi(\gamma-1)\,\Gamma_n/a_n^2\}}, \tag{4.30}$$

in which Γ_n is given by (4.9) with $a = a_n$ and ω_n is the adiabatic resonant frequency of a bubble of radius a_n.

Equation (4.30) is the dispersion relation governing the propagation of a plane wave of the form $e^{i(kx-\omega t)}$. When the bubbles all have the same radius, the

imaginary part of k determined by (4.30) is small except when the frequency ω of the sound wave is close to the resonance frequency of the bubbles, where it rises to a very sharp peak, corresponding to rapid attenuation of the wave. The magnitude of the peak is determined by the value of the thermometric conductivity. Of course, even in the case of a fairly moderate distribution of bubble sizes the summation in (4.30) tends to reduce considerably the size of the peak and extend it over a much wider range of frequencies. This probably accounts for the apparent discrepancy between the simple theory and the observed attenuation curves reported by Fox, Curley & Larson (1955). It is difficult to assess the importance of this broadening, but if it can be assumed that the distribution of bubble sizes is not too extensive, which is perhaps reasonable at the higher pressure ratios in view of the fairly constant observed resonance frequencies, it seems reasonable to suppose that the *ratio* of the peak attenuation coefficients for propagation through helium bubbles and air bubbles is still governed by the values of the corresponding conductivities.

In this case it is a relatively simple matter to deduce from (4.30) that near resonance

$$k_I \propto \{(\gamma-1)\sqrt{\chi}\}^{-\frac{1}{2}}, \tag{4.31}$$

where k_I is the imaginary part of k, the constant of proportionality being dependent on the frequency and bubble volume density. This implies that the attenuation distance of a wave is proportional to $\{(\gamma-1)\sqrt{\chi}\}^{\frac{1}{2}}$. Actually it should be mentioned that in all of these considerations we have ignored the attenuation which occurs because of *incoherent* scattering by the bubbles. But such scattering serves only to redirect the sound and does not represent a net loss of acoustic energy.

To interpret this result we now suppose that, when a large bubble disintegrates in the nozzle flow, only the resulting smaller bubbles located within a distance from the free surface of the jet proportional to $\{(\gamma-1)\sqrt{\chi}\}^{\frac{1}{2}}$ can effectively radiate into free space. Other things being equal this implies that the sound pressure level of the helium bubbles will exceed that of the air bubbles by

$$10\log_{10}\left\{\frac{(\gamma_{\mathrm{He}}-1)\sqrt{\chi_{\mathrm{He}}}}{(\gamma_{\mathrm{Air}}-1)\sqrt{\chi_{\mathrm{Air}}}}\right\} \simeq 6{\cdot}8\,\mathrm{dB}.$$

This is a remarkable prediction since it agrees very well with the observed relative levels (cf. figure 9*a*). In view of the approximations involved the agreement is perhaps fortuitous, nevertheless the implication is certainly that thermodynamic dissipation processes associated with the internal dynamics of the bubble response are indeed responsible for the observed differences.

5. Conclusion

The results of the experiment described in this paper lend strong support to the principle that a considerable reduction in the level of internally generated sound can be achieved by reducing as much as practicable the maximum pressure gradient in the nozzle. It appears that similar benefits should also be possible in

hot subsonic air jets, in which it is thought that the magnitude of the pressure gradient also controls the level of the excess noise. In this case, however, the acceleration of the flow in the turbine blade rows is probably more important than that in the nozzle, and it is hard to envisage how the local pressure gradient in the blade passages can be significantly modified, except perhaps by radical design changes such as increasing the chord or the number of turbine stages. The most efficient way to reduce the pressure gradient in the nozzle would be to modify the wall profile in the manner of the 'bellmouth' nozzle, and this could quite easily be incorporated into the design of a propulsion unit.

This paper documents a study undertaken as part of the Rolls-Royce (1971) Ltd programme of research into high speed jet noise.

REFERENCES

BATCHELOR, G. K. 1967 *An Introduction to Fluid Dynamics.* Cambridge University Press.

BATCHELOR, G. K. 1969 Compression waves in a suspension of gas bubbles in liquid. In *Fluid Dyn. Trans.* (ed. W. Fiszdon, P. Kucharczyk & W. J. Prosnak), vol. 4, p. 425. Warsaw: Polish Scientific Publishers.

CANDEL, S. M. 1972 Analytical studies of some acoustic problems of jet engines. Ph.D. thesis, Cal. Inst. Tech., Pasadena.

CARSTENSEN, F. L. & FOLDY, L. L. 1947 *J. Acoust. Soc. Am.* **19**, 481.

CHAPMAN, R. B. & PLESSET, M. S. 1970 Thermal effects in the free oscillation of gas bubbles. *Div. Engng Appl. Sci., Cal. Inst. Tech. Rep.* no. 85–50.

CRIGHTON, D. G. & FFOWCS WILLIAMS, J. E. 1969 *J. Fluid Mech.* **36**, 585.

CUMPSTY, N. A. 1974 Excess noise from gas turbine exhausts. *Aero. Res. Counc.* **35**, 726, N939.

CUMPSTY, N. A. & MARBLE, F. E. 1974 The generation of noise by the fluctuations in gas temperature into a turbine. *Cambridge University, Engng Lab. Rep.* CUED/A TURBO/ TR57.

DEVIN, C. 1959 *J. Acoust. Soc. Am.* **31**, 1654.

DILS, R. R. 1973 Dynamic gas measurements in a gas turbine transition duct exit. *A.S.M.E. Paper*, no. 73–GT–7.

DOWLING, A. 1976 *J. Fluid Mech.* **74**, 529.

FFOWCS WILLIAMS, J. E. & HOWE, M. S. 1975 *J. Fluid Mech.* **67**, 597.

FFOWCS WILLIAMS, J. E., SIMSON, J. & VIRCHIS, V. 1975 *J. Fluid Mech.* **71**, 251.

FOX, F. E., CURLEY, S. R. & LARSON, G. S. 1955 *J. Acoust. Soc. Am.* **27**, 534.

HALL, L. H. 1969 Flow noise. Ph.D. thesis, Imperial College, London.

HINZE, J. O. 1955 *A. I. Ch. E. J.* **1**, 289.

HOCH, R. & HAWKINS, R. 1973 Recent studies into Concorde noise reduction. *AGARD Conf. Proc.* no. 131, paper 19.

HOWE, M. S. 1975 *J. Fluid Mech.* **71**, 625.

LIGHTHILL, M. J. 1952 *Proc. Roy. Soc.* A **221**, 564.

MACPHERSON, J. D. 1957 *Proc. Phys. Soc. Lond.* B **70**, 35, 1953.

MEYER, E. & SKUDRZYK, E. 1953 *Akust. Beihefte*, **3**, 434.

MINNAERT, M. 1933 *Phil. Mag.* **16**, 235.

MORFEY, C. L. 1973 *J. Sound Vib.* **31**, 391.

PICKETT, G. F. 1974 Turbine noise due to turbulence and temperature fluctuations. *Paper 8th Int. Cong. Acoustics, London.*

SILBERMAN, E. 1957 *J. Acoust. Soc. Am.* **29**, 925.

STRASBERG, M. 1953 *J. Acoust. Soc. Am.* **25**, 536.

STRASBERG, M. 1956 *J. Acoust. Soc. Am.* **28**, 20.

TANGREN, R. F., DODGE, C. H. & SEIFERT, H. S. 1949 *J. Appl. Phys.* **20**, 637.

WALLIS, G. B. 1969 *One-Dimensional Two-Phase Flow.* McGraw-Hill.

WHITFIELD, O. J. 1975 Novel schemes for jet noise control. Ph.D. thesis, Engineering Department, University of Cambridge.

WIJNGAARDEN, L. VAN 1972 One-dimensional flow of liquids containing small gas bubbles. *Ann. Rev. Fluid Mech.* **4**, 369.

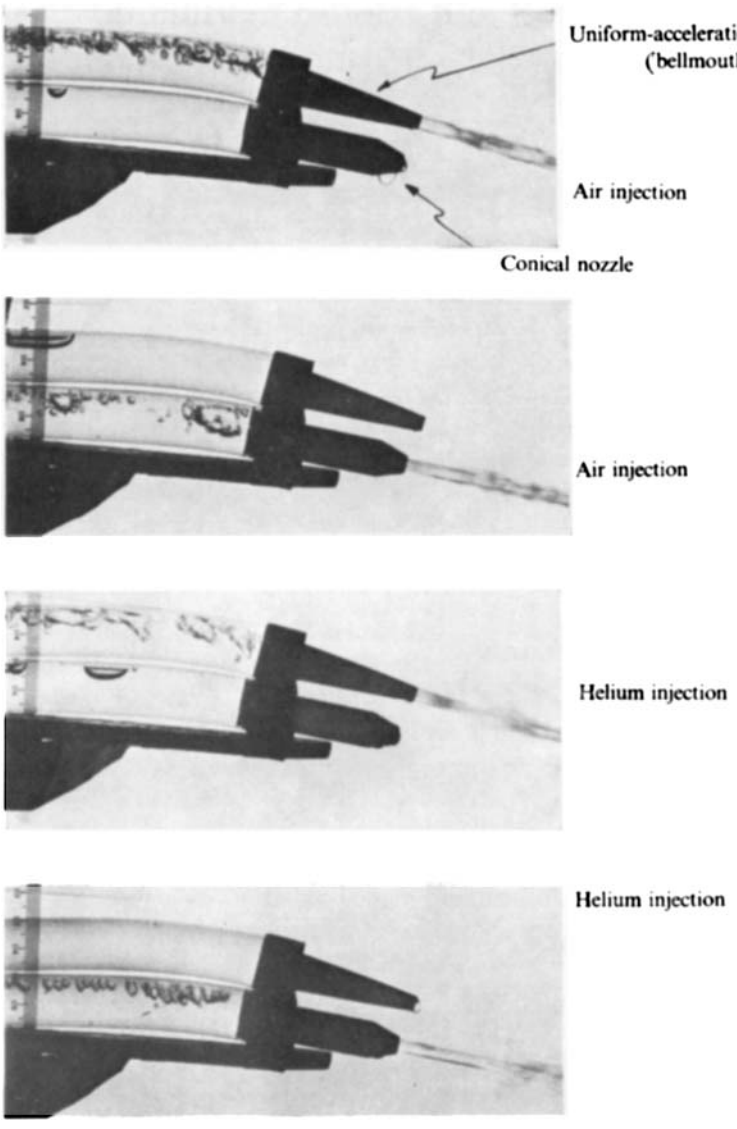

FIGURE 7. Photographs of two-phase flow entering the nozzles.
Nozzle pressure ratio = 1·68.

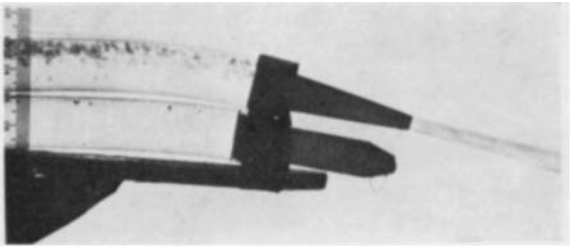

Air injection

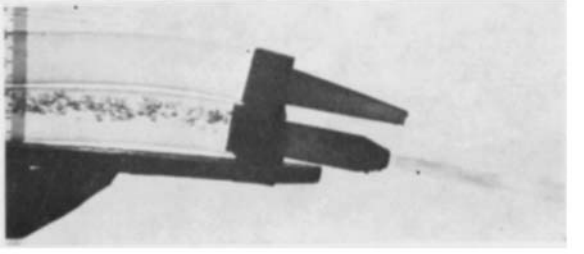

Air injection

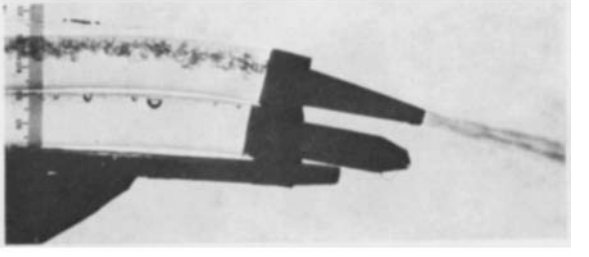

Helium injection

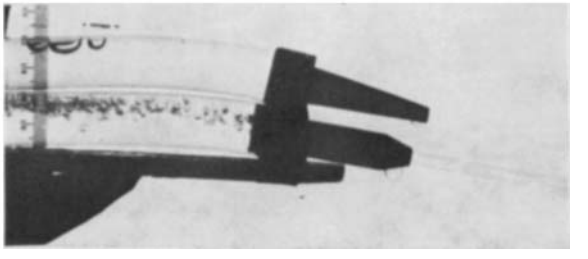

Helium injection

FIGURE 8. Photographs of two-phase flow entering the nozzles.
Nozzle pressure ratio = 3·04.